

# Large-area electronics enabled high resolution digital microfluidics for single cell manipulations

Siyi HU<sup>1</sup>, Jingmin YE<sup>2</sup>, Subao SHI<sup>2</sup>, Kai JIN<sup>1</sup>, Dongping WANG<sup>1</sup> & Hanbin MA<sup>1,2\*</sup>

<sup>1</sup>CAS Key Laboratory of Bio-Medical Diagnostics, Suzhou Institute of Biomedical Engineering and Technology, Chinese Academy of Sciences, Suzhou 215163, P.R.China

<sup>2</sup>Guangdong ACXEL Micro & Nano Tech Co., Ltd, Guangdong province, 528000, P.R.China

**Author contributions:** S.H and H.M conceived the concept and experiments. S.H, J.Y, S.S and D.W performed the research. S.H, K.J and D.W analyzed the data. S.H, D.W and H.M wrote the paper.

## Abstract

Thin-film semiconductor devices as switching elements are perfect fit for electrodes-array based digital microfluidics. With support of large-area electronics technology, high-resolution digital droplets (diameter around 100  $\mu\text{m}$ ) contains single cell can be generated by pre-programmable addressing signals. Single-cell generation and manipulation is a foundation of single-cell research, which demands ease of operation, multifunctional and accurate tools. Herein, we report an active-matrix digital microfluidic platform for single-cell generation and manipulation enabled by large-area electronics technology. The active device contains 26,368 electrodes that can be independently addressed to perform parallel and simultaneous droplets and even single cells manipulation. An on-chip generated single droplet volume limit of 500 pL has been reported, proving the continuous and stable movement of the droplet containing cells for over 1 hour. Furthermore, the success rate of single droplet formation can be higher than 98% and able to generate around 10 single cells within 10 seconds. A pristine single cell generation rate of 29% is achieved without any further sorting process

**Keywords:** Digital microfluidics; Active-matrix; Single cell manipulation; Large-area;

## 1. Introduction

Due to the heterogeneity of cells in biological sciences, medicine, and biology, it is often necessary to sort out the single cells we need from more complex samples and conduct subsequent scientific research or industrial production. Such as, in cancer research, we need to sort out the single cancer cell, which is the premise of subsequent single-cell sequencing (1-3). In the biomanufacturing cell line, first sort out a single cell that can derive subclones, which is the following guarantee of the cell line prerequisite for stable acquisition (4, 5). However, the volume of single cells is relatively small, typically around the scale of nanoliters or picolitres, which is difficult to achieve precise control by conventional laboratory methods. A complete single-cell analysis process typically requires three main steps: 1) cell manipulation, such as cell capture, selection, or sorting; 2) cell processing, such as transfection, injection, or lysis; 3) detection of the physical and chemical properties, homeostatic conditions or functional reactions. Overall, the current single-cell research is still in its infancy, mainly limited by the single-cell platform technology, making many of the advantages of single-cell research unable to play (6, 7).

Therefore, according to the development needs of single-cell research, many solutions for single-cell sorting and manipulation have emerged. Microfluidic technology, which can handle microliter or even nanoliter level liquid manipulation, has developed into a platform-level and evolving single-cell manipulation and analysis technology (8-10). Microfluidic technology has many advantages that conventional benchtop laboratory methods cannot match. Among them, for cell sorting and manipulation, different microfluidic ways have gradually been discovered and applied by researchers, including fluid mechanics (11), electrical (12-14), optical (15-17), magnetic (18) and acoustic (19, 20) methods. The electrowetting-on-dielectric (EWOD) digital microfluidic (DMF) technology based on electricity can realize the free manipulation of nanoliter or even picolitre droplets in a two-dimensional plane (21, 22), making it a most promising technology platform for single-cell sorting and manipulation. EWOD DMF technology has demonstrated a unique ability to integrate downstream analysis with single-cell sorting and manipulation in applications compared to other microfluidic technologies (13, 23). The parallel plate structure of the EWOD-DMF system allows it to easily integrate real-time feedback technology in a relatively large area according to its optical or electrical properties (14, 24-27). In single-cell research applications, high-throughput single-cell parallelism can be realized to manipulate and analyze and enable the development of multiple time- and space-resolved analysis methods. Many studies have demonstrated that the EWOD DMF technique can be applied to analyze suspended or single adherent cells (13, 23, 28). However, the studies are mainly based on DMF chips with arrays of passive electrodes (29), i.e., each electrode is physically connected to a peripheral switch. The total number of electrodes allowed by DMF systems is typically less than 200. The scalability has become a true obstacle for this technology to be used in single-cell research development (30, 31).

Active-matrix (AM) technology, which integrates thin-film transistor into each pixel to achieve pixel control in a large array, widely used in flat panel displays (32). AM technology in EWOD would be an ideal solution to overcome the limitation of the passive electrode array (33, 34). A few groups have applied AM-DMF in molecular diagnosis (35, 36), but there are few reports on its application in the study of single-cell applications. In order to generate a single cell contained tiny droplet, the resolution of EWOD electrodes and the droplet diameter need to reach around 100  $\mu\text{m}$  scale (which is one magnitude bigger than the diameter of a typical mammal cell). This rigorous requirement could only be achieved when the pixel circuits, drive signals and materials combination of an AM-DMF device are carefully optimized. In this work, we report an AM-DMF platform for high efficiency single cell generation and manipulations. The platform provides a unique solution

to the problem of efficiently obtaining single-cell samples in the current development of single-cell research. This method can be extended and universally used in single-cell analysis research and can be integrated with many single-cell research tools to obtain single-cell information and application in multiple dimensions.

## **2. Methodology**

### **2.1 AM-DMF chip design and fabrication**

The chip design is shown in Fig 1 (b)-(d), the bottom glass plate with thin film transistor (TFT) electrode array was fabricated on a 0.5mm glass substrate by LCD manufacturing process, which produced by the Tianma Micro-electronics (Shenzhen, China). The complete AM-DMF chip contains an AM-DMF device array, a spacer, a conductive top plate with the hole for liquid sample injection. The cross-section view of the chip as shown in Fig S1, the AM-DMF array we get from the Tianma was already with 1T-1C pixels, an electrowetting dielectric layer of 300 nm SiNx, then spin coat the hydrophobic layer in our own laboratory. The hydrophobic layer we mainly test CYTOP (from Asahi Glass Company) dissolved in different solvents, which is FC43 (from 3MTM), KBE-903 (from Shin-Etsu Chemical), Solv 180 (from Asahi Glass Company) and another kind of hydrophobic layer material Teflon (from Chemours Company), as shown in Fig2(b). The plastic spacer was applied to define the gap of 30 $\mu$ m between the top ITO coated top glass plate and the bottom plate. The ITO layer on ITO glass cover is also spin coated with a hydrophobic layer, and the top and bottom hydrophobic layers are encapsulated facing to each other during encapsulation. The conductive ITO is connected to the system ground through silver glue. The custom designed FPC was then attached to the chip for the connection with the control board. The AM-DMF chip assembly and final cartridge construction as shown in Fig S1.

### **2.2 The AM-DMF system setup**

The AM-DMF system contained four main parts, which are the AM-DMF chip, the electronic control board, the customer-written control software and the optical detection model, as shown in Fig S2. The AM-DMF chip was fixed in the 3D-printed test fixture holder, which contain the electronic control board. The software was applied to acquire the droplets generation and position, which has functions such as drive signal modulation (such as voltage, frequency and time etc.), droplet motion path generation and execution, etc. For the optical detection system, we setup by ourselves. The main frame, imaging tube, narrow-band filter, dichroic lens, etc. were all purchased from Thorlabs Inc. And the microcopy object lens purchased from the Nikon Inc. The imaging camera we applied is the sCMOS camera (C13440, Hamamatsu, Japan).

### **2.3 Reagents**

Ethanol, acetone, IPA were all purchased from the Sinopharm Chemical Reagent Ltd Co, which mainly applied to washing the chip. Silicone oil (5 cSt) and the surfactant Pluronic F68 was purchased from Sigma Aldrich (Oakville, ON, USA). The HEK 293 cell were obtained from the American Type Culture Collection (Manassas, VA, USA). Modified Eagle's Medium (MEM), fetal bovine serum (FBS), trypsin-EDTA and phosphate buffer solution (PBS) were purchased from Gibco. Cell viability was determined using a calcein/propidium iodide dual-staining assay (Invitrogen, Molecular Probes). All chemicals were used as received without further purification. The deionized (DI, 18.2 M $\Omega$  cm) water used in all the studies was purified using a Milli-Q water purification system.

## 2.4 Cell Culture

The HEK 293 cells were cultured in a cell culture incubator (5% CO<sub>2</sub>, saturated humidity, 37 °C). The growth medium for the HEK 293 cell was MEM containing 10% of FBS, 100 µg/mL of penicillin, and 100 µg/mL of streptomycin. The cell lines were cultured every 2-3 days for each passage at 105 cells/mL per cm<sup>2</sup>. Prior to the experiments, the cells were dissociated and resuspended in a fresh whole medium. The number of cells and cell viability were measured by cell counting plate (177-112C, Waston, Japan) and calcein/propidium iodide dual-staining assay kit.

## 2.5 Single Cell manipulation on the AM-DMF chip

Before the experiment begins, it is necessary to start the software to establish communication with the AM-DMF chip hardware system, and edit the single-cell droplets generation path based on the One-to-Two method on the software. Then, the silicone oil is injected into the chip through the injection hole for use. Next, we prepared the cell suspension for single-cell sorting. First, the cells were digested from the culture flask with trypsin. After centrifugation at 1000 rpm for 5 min, the supernatant was removed, and the cells were resuspended in 1 mL of PBS. Then we count the cells, and we need to configure four concentrations of cell suspensions according to the experimental requirements, which are 105, 5×10<sup>4</sup>, 10<sup>4</sup>, and 5×10<sup>3</sup> cells/mL. Next, we need to add 0.01% (v/v) F68 surfactant to the cell suspension, so that the cells can move more stably in the AM-DMF chip. Then we run the sample injection program on the software, that is, apply a driving voltage to the electrodes around the sample injection port, so that the electrodes around the sample injection port have hydrophilic properties and facilitate the smooth loading of the cell suspension. In addition, the live-cell tracer dye analysis method was used to analyze the cell viability on- and off-chip. Then we started running the automated path for cell sorting, enabling single-cell droplet generation. In this study, we repeated each single-cell droplet generation experiment more than three times.

## 3. Results

### 3.1 Cartridge, control system development of AM-DMF system

To build a platform for efficient and high-throughput single-cell sample preparation that integrates the function of single-cell sorting, manipulation, parallel automated manipulation of picolitre volume droplet and optical detection. Here we developed an AM-DMF system to solve the problem of single-cell sorting and manipulation, as shown in Fig 1. The AM-DMF chip consists of two parallel glass plates, which is the bottom glass plate has a thin film transistor (TFT) electrode array, and the upper glass plate is ITO conductive glass with sample injection holes. The upper and bottom layers are separated by a gap spacer (Fig S1). For the bottom active electrode array, we designed 8 groups of parallel regions, which increased the scale of the overall array and reduced the number of signal lines, as shown in Fig 1(b). With 64 row signals and 64 column signals, a total of 26,368 electrodes can be controlled independently. According to the requirements of the droplet generation method and volume, we mainly use three kinds of electrode designs, which are divided into square and hexagonal in shape, which are mainly 125µm and 250µm in size (Part A, B, C in Figure 1(b) and Table S1). Each pixel contains a TFT and a capacitor, forming a 1T1C circuit. EWOD electrodes can be charged and discharged by

row and column scanning. The minimum size of the electrode is  $125\mu\text{m} \times 125\mu\text{m}$ . When we use a spacer of  $30\mu\text{m}$  for the gap, the droplet manipulation with a minimum volume of about 500pL can be achieved to meet the volume requirements for single-cell droplet manipulation. Based on the need of generating single-cell droplets, we design the electrode arrangement of pixel electrodes of different shapes and sizes according to three functional areas: cell loading, cell droplet split, and single-cell droplet generation, and finally form an AM-DMF system for the application of single-cell. The core assembly is a substrate with an active electrode array. The upper ITO glass substrate acts as a ground electrode.

The above mainly introduces the core components of AM-DMF. To form the whole system, we also design and manufacture the main control board, including a micro-controller (MCU), power supply and row and column address controller (multiplexer). The control board is connected with the AM-DMF chip through a flexible printed circuit (FPC). At the same time, we also integrated a large field of view microscopic optical imaging system above the AM-DMF chip for real-time monitoring and imaging of the experimental process. And we have designed the software control system by ourselves, which can communicate continuously with the main control board and perform automatic process editing and real-time control of the experimental process (Fig S1).

### 3.2 AM-DMF system characterization for the single cell manipulation

To achieve stable manipulation of cell-containing liquid samples on AM-DMF chip, such as liquid distribution, droplet generation, droplet movement, etc., we need to optimize and select relevant parameters that affect droplet movement. Previous studies (32) have shown that the array drive sequence of the AM chips used in our study is similar to that of a standard flat-panel display. The serial of the SCAN signal mainly performs the row selection, and the parallel of the DATA signal sets the column signal. Our previous research obtained that when the SCAN period is set to  $100\mu\text{s}$  and DATA is set to  $110\mu\text{s}$ , the off-set is  $10\mu\text{s}$ , and the refresh rate of the array is 160ps. At the same time, combined with the simulation data, when  $V_{\text{data}}$  is 40V, and  $V_{\text{scan}}$  is 50V, the charging and discharging of the pixel is simulated, and the window of the pixel-on is obtained enough to match the driving needs (Fig 2a).

After the driving parameters are determined, for the chip hardware, parameters such as the hydrophobic layer of the chip, the gap between the top and bottom plate, and the related properties of the droplet itself become the main factors affecting the movement of the droplet. When the characteristic size of the droplet is reduced to the nanoliter or even picoliter level, the properties of the microdroplet will change, and the size effect of the microdroplet will occur. As the size of the microdroplets decreases, the surface area to volume ratio becomes larger and larger, that is, the larger the specific surface area, the microdroplets exhibit surface effects. The size effect relationships for various forces and feature sizes are not equal. When the feature size decreases, the body force decreases faster than the adhesion force, and the adhesion force

replaces the effect of the body force and becomes the dominant force for the movement of the droplet. For microliter-scale droplets, surface tension dominates among the three adhesion forces. Compared with Van der Waals and electrostatic forces, changing the surface tension to drive the microdroplets is the easiest to implement. Based on the classical Young's equation (as shown in Supplementary Materials) used to describe the wetting characteristics of the solid-liquid-gas three-phase interface, the wetting level of the droplet is also closely related to the surface tension of the liquid, gas and solid three-phase interface. At the same time, according to the Young-Laplace formula (as shown in Supplementary Materials), the relationship between the gas-liquid interface pressure difference and the surface tension can be seen. Therefore, the above two equations constitute the fundamental equation of surface tension drive. Therefore, the method of changing the droplet's surface tension is based on the generation method and working principle. In applying DMF technology, we mainly use two methods of adding special reagents to the microdroplet and surface modification. Surface modification mainly refers to the surface treatment of the chip substrate material to change the surface tension to form a gradient by modifying the wetting of the solid surface.

We also tested the contact angle changes of different functional regions under the action of driving signals (Fig 2 (c)-(e)). We selected three commonly used reagents, deionized water (DI water), phosphate buffered saline (PBS), and serum-free media (MEM) for testing. The test volume was about  $0.5\mu\text{L}$ . The reagents were placed in a silicone oil medium, and a tungsten alloy probe was inserted on the droplet as a ground electrode. The initial contact angles are all around  $170^\circ$ , and the contact angles decrease with the increasing DATA voltage. We have further compared the three regions A, B, and C. When the same DATA voltage is applied, the contact angle of the larger electrode corresponding to the region C is smallest, and the control force on the droplet is stronger. This phenomenon may be because the effect of edge charges in the large electrode is more obvious, which promotes the larger surface tension of the large electrode.

Based on the above principles, we tested the contact angles of liquid reagents on different hydrophobic coatings that we would involve in single-cell sorting and manipulation tests. The liquid reagents including DI water, PBS, serum-free media (MEM), serum-containing media (MEM+FBS) and cell-containing solutions (Cell). The hydrophobic coating is based on the previous research foundation and literature research (27, 31, 33), and mainly selects Teflon and CYTOP, two commonly used hydrophobic coatings for EWOD. For CYTOP, we tested CYTOP dissolved in four different solvents. We use  $0.5\mu\text{L}$  of droplets for the test droplets, the test results show that the contact angle of Teflon for various liquid reagents is larger than that of other hydrophobic coatings, especially the contact angle of the liquid containing cells on the surface of Teflon is much larger than those of other hydrophobic coatings, so we will test in the following



experiments. The hydrophobic coatings of both the upper and bottom plates are made of Teflon layer, and here we use spin coating to modify the hydrophobic coatings.

The stability of droplet movement and generation is the leading indicator for evaluating the performance of the AM-DMF chip. We selected commonly used biological solvents as test samples, including DI water, PBS, MEM and MEM with serum (with 0.01% F68 surfactant, MEM+FBS(F68)). Previous studies have shown that a certain amount of surfactant can be added to biological reagents containing proteins, thereby improving their mobility stability and reducing the adsorption of proteins on the electrode surface. For the stability of droplet movement, we selected a row of 5 electrodes in area A, let a single droplet make a continuous reciprocating motion on these 5 electrodes, and video-monitored the movement state. The test results are shown in Fig. 3(a), in addition to MEM solvent, the other three solvents can achieve continuous movement for more than 1 hour when the forms mentioned above of exercise are repeated and can maintain a good movement form, among which PBS and MEM+FBS(F68) are the main solvents for single-cell experiments. In addition, the stability of droplet generation is also a parameter that we need to verify. We chose the "One-to-Two" method to generate a single droplet in region A in this work. The final droplet generated is one droplet controlled by two electrodes, and the volume of each droplet is about 1nL. This "One-to-Two" method can efficiently and quickly divide a large droplet into multiple small droplets to form a regularly arranged droplet matrix, which is more suitable for high-throughput large-scale single-cell droplet generation and sorting. We tested 32 droplet generation tests for each solvent through the pre-edited automatic droplet generation, and we tested each reagent more than 3 times, the test results are shown in Fig 3(b). The results show that the probability of generating 32 droplets of the above solvents is greater than 82%, that is, more than 26 effective single droplets can be obtained at a time. Among them, the probability of single droplet generation of PBS is close to 100%, reflecting the high stability of single droplet generation. The above also proves that the "One-to-Two" droplets generation path that we have chosen is effective.

### 3.3 Single Cell generation and manipulation on the AM-DMF chip

Once we have identified the hydrophobic coating and solvent, we need to determine and optimize the conditions for single-cell droplet generation. To generate a large number of droplets in a short time, we chose this "One-to-Two" droplet generation method, as shown in Fig. 4(a). This droplet generation method enables exponential growth in the number of individual droplets. Compared with the single-cell droplet generation method in traditional microchannels, this method of single-cell droplet generation on the AM-DMF chip is not limited by physical microchannels and structures, which further restricts the movement path and volume of droplets. Moreover, each single-cell droplet generated can be assigned an electronic code without the traditional barcode, and the target single-cell droplet can be individually manipulated through the

EWOD electrode. At the same time, the precise control of droplet volume can be achieved through the EWOD electrode. Therefore, this AM-DMF system-based "One-to-Two" droplet generation method is more efficient and flexible than the traditional droplet generation method. Applying this "One-to-Two" automated droplets generation approach, we successfully achieved the automatic generation of 32 droplets from the cell-containing suspension at the A region. The generation from a single droplet to 32 droplets took 8 seconds after 5 steps of splitting operations, as shown in Fig 4(b) and Movie S1. We then identified droplets containing single cells from the fluorescence microscopic images (Fig 4(b)), it can be clearly seen from the fluorescence microscopic image that the droplet contains one single cell. We can select a target droplet containing a single cell according to research acquirement and move the droplet containing the single cell freely in a directional manner. We can move them out to the idle electrode area, where other single-cell-based operations could be performed, as shown in Movie S2. Suppose the cell sample is relatively rare and precious. In that case, we can also collect and recover droplets containing multiple cells in situ, then perform droplet generation, and so on, until the obtained droplets are all single-cell droplets, which is also what the traditional microfluidic systems cannot achieve.

To efficiently obtain droplets containing a single cell, the initial concentration of the cells is also an important parameter. Therefore, we tested cell suspensions with four concentration gradients and compared their effective droplet generation probability and the probability that the generated droplets contain single-cell droplets, and the results are shown in Fig 4(c). We can see that the effective generation probability of droplets is close to 100%, which proves that the droplet generation path and driving parameters are stable and accurate. When the cell concentration was reduced from  $10^5$  cells/mL to  $10^4$  cells/mL, the probability of obtaining a single droplet containing a single cell increased from 3.1% to 43.3%. As the cell density continued to decrease to  $5 \times 10^3$  cells/mL, the probability that the droplet contained a single cell decreased. Therefore, based on the experimental results, 104 cells/mL was used as the optimized cell concentration for single-cell generation in the following experiments.

Then we selected the HEK 293 cell suspension with a concentration of  $10^4$  cells/mL. Under the conditions that the driving signal  $V_{\text{scan}}$  is 40V,  $V_{\text{data}}$  is 30V, the holding time is 100 $\mu$ s, and the delay time is 1000 $\mu$ s, the "One-to-Two" automatic path was applied. Generation of 32 droplets was performed to obtain droplets containing single cells. We got the results shown in Fig 5(a) and Fig S3 by repeating the test experiment 5 times. It can be seen that the average probability of successfully generating 32 single droplets is 98.8%, which has a high success rate and can meet the needs of single-cell droplet generation. The probability of containing single-cell droplets is 29.7%, which has exceeded the probability of obtaining single-cell droplets in some traditional microfluidic systems and has met the needs of existing single-cell omics research. After demonstrating that single-cell droplets can be generated and manipulated using AM-DMF chips,



we also investigated the effects of AM-DMF on cell viability, the results as shown in Fig 5(b). Here we applied for electrodes to drive one single droplet, and the volume of a single droplet is 2nL. We proved that the cells manipulated by the DMF chip still have good cell viability through living cell tracer dye. The results show that the green fluoresce signal means the cell is living, and the red signal means the cell is dead. The above studies have proved that our AM-DMF chip can generate droplets containing single cells with high efficiency and high throughput, and the system has good biocompatibility. It maintains good activity and can be directly used for subsequent single-cell research applications, which makes up for the shortcomings that some existing single-cell sorting methods will damage cells.

#### 4. Discussion and Conclusion

Although the existing single-cell sorting and analysis platforms can rapidly acquire single cells, and the manipulation of single cells can be achieved with optical, magnetic and acoustic technologies, the complexity of the existing methods limits the high throughput parallel acquisition. Typically, devices or equipment with high throughput function of single-cell have relatively complex structures, it is not easy to integrate with the related single-cell analysis technology, thus limiting the promotion and development of the single-cell analysis system. The AM-DMF we developed can simplify the single-cell acquisition process, realising high-throughput parallel manipulation of nanoliter or even picoliter single-cell droplets. And also can replace the traditional approach of adding barcodes by assigning addressable electronic codes, further simplify the experimental steps for single-cell sorting. The AM-DMF technology platform can realise high-throughput single-cell sorting and the free manipulation of single cells on a two-dimensional plane based on the EWOD principle, because each of our EWOD electrodes can be independently manipulated. And our AM-DMF technology platform is different from the passive DMF technology platform. The existing passive DMF platform is limited by hardware and manufacturing process. At present, the maximum number of control electrodes is not more than 200, and it is limited by the space for the arrangement of electrodes and wires. Due to limitations, it is not easy to achieve a large-area matrix electrode arrangement. We can currently support 26,368 electrodes on the AM-DMF technology platform. More than 1000 single cells can be processed in parallel on a single chip when all electrodes are rationally utilized. They can be easily combined with optical detection, magnetic attraction, temperature control modules. The functions such as editing, culture, and molecular detection based on single cells even can be expanded and integrated in the future. Faced with the need for high-throughput single-cell sorting, manipulation, and enrichment processes in digital cell biology derived from single-cell omics, AM-DMF will be a very promising technology. We expect that, with the technology introduced here and the subsequent continuous improvement and enrichment of matching functional modules, AM-DMF can serve as a powerful single-cell sample processing platform to achieve more applications based on single-cell omics, while also enabling this platform technology extends to many research areas such as biological sciences and chemistry.

## ACKNOWLEDGEMENTS

General: The authors thank Linkzill Technology Co., Ltd. and TIANMA microelectronics Corp for the a-Si:H TFT array design and fabrication.

Funding: This research was funded by Science and Technology Innovation Project of Foshan, Guangdong Province, China (Grant No.1920001000047).

## References

1. J. Lee, D. Y. Hyeon, D. Hwang, Single-cell multiomics: technologies and data analysis methods. *Experimental & Molecular Medicine* **52**, 1428-1442 (2020).
2. B. Lim, Y. Lin, N. Navin, Advancing Cancer Research and Medicine with Single-Cell Genomics. *Cancer Cell* **37**, 456-470 (2020).
3. X. Xu *et al.*, Microfluidic Single-Cell Omics Analysis. *Small* **16**, 1903905 (2020).
4. L. P. Pybus *et al.*, Coupling picodroplet microfluidics with plate imaging for the rapid creation of biomanufacturing suitable cell lines with high probability and improved multi-step assurance of monoclonality. *Biotechnology Journal* **17**, 2100357 (2022).
5. S. H. Gohil, J. B. Iorgulescu, D. A. Braun, D. B. Keskin, K. J. Livak, Applying high-dimensional single-cell technologies to the analysis of cancer immunotherapy. *Nature Reviews Clinical Oncology* **18**, 244-256 (2021).
6. B. Korin, J.-J. Chung, S. Avraham, A. S. Shaw, Preparation of single-cell suspensions of mouse glomeruli for high-throughput analysis. *Nature Protocols* **16**, 4068-4083 (2021).
7. H. Keren-Shaul *et al.*, MARS-seq2.0: an experimental and analytical pipeline for indexed sorting combined with single-cell RNA sequencing. *Nature Protocols* **14**, 1841-1862 (2019).
8. E. Rosàs-Canyelles, A. J. Modzelewski, A. Geldert, L. He, A. E. Herr, Assessing heterogeneity among single embryos and single blastomeres using open microfluidic design. *Science Advances* **6**, eaay1751 (2020).
9. B. B. Yellen *et al.*, Massively parallel quantification of phenotypic heterogeneity in single-cell drug responses. *Science Advances* **7**, eabf9840 (2021).
10. C. Clark Iain *et al.*, Barcoded viral tracing of single-cell interactions in central nervous system inflammation. *Science* **372**, eabf1230 (2021).
11. L. Mazutis *et al.*, Single-cell analysis and sorting using droplet-based microfluidics. *Nature Protocols* **8**, 870-891 (2013).
12. J. Lamanna *et al.*, Digital microfluidic isolation of single cells for -Omics. *Nature Communications* **11**, 5632 (2020).
13. Q. Ruan *et al.*, Digital-WGS: Automated, highly efficient whole-genome sequencing of single cells by digital microfluidics. *Science Advances* **6**, eabd6454 (2020).
14. A. H. C. Ng, M. D. Chamberlain, H. Situ, V. Lee, A. R. Wheeler, Digital microfluidic immunocytochemistry in single cells. *Nature Communications* **6**, 7513 (2015).
15. S. Zhang *et al.*, Reconfigurable multi-component micromachines driven by optoelectronic tweezers. *Nature Communications* **12**, 5349 (2021).
16. P. Y. Chiou, A. T. Ohta, M. C. Wu, Massively parallel manipulation of single cells and microparticles using optical images. *Nature* **436**, 370-372 (2005).
17. K. Le *et al.*, Assuring Clonality on the Beacon Digital Cell Line Development Platform. *Biotechnology Journal* **15**, 1900247 (2020).
18. W. Yu *et al.*, A ferrobotic system for automated microfluidic logistics. *Science Robotics* **5**, eaba4411 (2020).
19. P. Zhang *et al.*, Acoustic streaming vortices enable contactless, digital control of droplets. *Science Advances* **6**, eaba0606 (2020).

20. S. P. Zhang *et al.*, Digital acoustofluidics enables contactless and programmable liquid handling. *Nature Communications* **9**, 2928 (2018).
21. R. Wheeler Aaron, Putting Electrowetting to Work. *Science* **322**, 539-540 (2008).
22. M.-Y. Chiang, Y.-W. Hsu, H.-Y. Hsieh, S.-Y. Chen, S.-K. Fan, Constructing 3D heterogeneous hydrogels from electrically manipulated prepolymer droplets and crosslinked microgels. *Science Advances* **2**, e1600964 (2016).
23. B. Li Bingyu *et al.*, Cell invasion in digital microfluidic microgel systems. *Science Advances* **6**, eaba9589 (2020).
24. L. Malic, T. Veres, M. Tabrizian, Nanostructured digital microfluidics for enhanced surface plasmon resonance imaging. *Biosensors and Bioelectronics* **26**, 2053-2059 (2011).
25. I. Swyer *et al.*, Digital microfluidics and nuclear magnetic resonance spectroscopy for in situ diffusion measurements and reaction monitoring. *Lab on a Chip* **19**, 641-653 (2019).
26. H. C. Ng Alphonsus *et al.*, A digital microfluidic system for serological immunoassays in remote settings. *Science Translational Medicine* **10**, eaar6076 (2018).
27. C. Zhang *et al.*, An Impedance Sensing Platform for Monitoring Heterogeneous Connectivity and Diagnostics in Lab-on-a-Chip Systems. *ACS Omega* **5**, 5098-5104 (2020).
28. J. Zhai *et al.*, A digital microfluidic system with 3D microstructures for single-cell culture. *Microsystems & Nanoengineering* **6**, 6 (2020).
29. J. Li, C.-J. C. Kim, Current commercialization status of electrowetting-on-dielectric (EWOD) digital microfluidics. *Lab on a Chip* **20**, 1705-1712 (2020).
30. L. Coudron *et al.*, Fully integrated digital microfluidics platform for automated immunoassay; A versatile tool for rapid, specific detection of a wide range of pathogens. *Biosensors and Bioelectronics* **128**, 52-60 (2019).
31. K. Jin *et al.*, “One-to-three” droplet generation in digital microfluidics for parallel chemiluminescence immunoassays. *Lab on a Chip* **21**, 2892-2900 (2021).
32. H. Ma *et al.*, in *2020 IEEE International Electron Devices Meeting (IEDM)*. (2020), pp. 35.35.31-35.35.34.
33. C. Hu, H. Zhang, C. Jiang, H. Ma, A geometrical model of pinch-off in digital microfluidics underpins “one-to-three” droplet generation. *Applied Physics Letters* **120**, 121602 (2022).
34. Y. Xing *et al.*, A robust and scalable active-matrix driven digital microfluidic platform based on printed-circuit board technology. *Lab on a Chip* **21**, 1886-1896 (2021).
35. B. Hadwen *et al.*, Programmable large area digital microfluidic array with integrated droplet sensing for bioassays. *Lab on a Chip* **12**, 3305-3313 (2012).
36. S. Anderson, B. Hadwen, C. Brown, Thin-film-transistor digital microfluidics for high value in vitro diagnostics at the point of need. *Lab on a Chip* **21**, 962-975 (2021).

## SUPPORTING INFORMATION

Young's equation

$$\cos\theta = \frac{\gamma_{sg} - \gamma_{sl}}{\gamma_{lg}}$$

Among them,  $\theta$  indicates that the contact angle is the angle between the tangent line and the contact surface between the liquid droplet and the solid. Contact angle describes the wetting properties of droplets to solid interfaces. The  $\gamma_{sg}$ ,  $\gamma_{sl}$  and  $\gamma_{lg}$  represent the surface tension of solid-gas, solid-liquid and liquid-gas, respectively. The value of  $\gamma_{sg}$ ,  $\gamma_{sl}$  and  $\gamma_{lg}$  determines the size of  $\theta$ .

Young-Laplace formula

$$\Delta P = \gamma_{lg} \left( \frac{1}{R_1} + \frac{1}{R_2} \right)$$

Among them, P is the pressure difference generated by the contact surface between the body and the droplet,  $\gamma_{lg}$  is the surface tension of the contact surface between the gas and the droplet, and  $R_1$  and  $R_2$  is the radius of curvature of the contact surface between the droplet and the gas phase. Therefore, as long as  $\gamma_{lg}$  is changed, a surface tension gradient is formed, resulting in different pressure differences between the two ends of the droplet, resulting in a difference in contact angle between the two ends of the droplet. The change of the contact angle at both ends will make the droplet along the contact angle smaller direction to move.

Table S1. Summary of pixel parameter.

Area	Pixel Shape	Pixel Size	Pixel Number	Storage Capacitor	Droplet Volume @Gap=30μm
A	Hexagon	288um	2048	4.34pF	2.2nL
B	Hexagon	144um	4096	4.08pF	0.55nL
C	Square	125um	16384	3.78pF	0.47nL

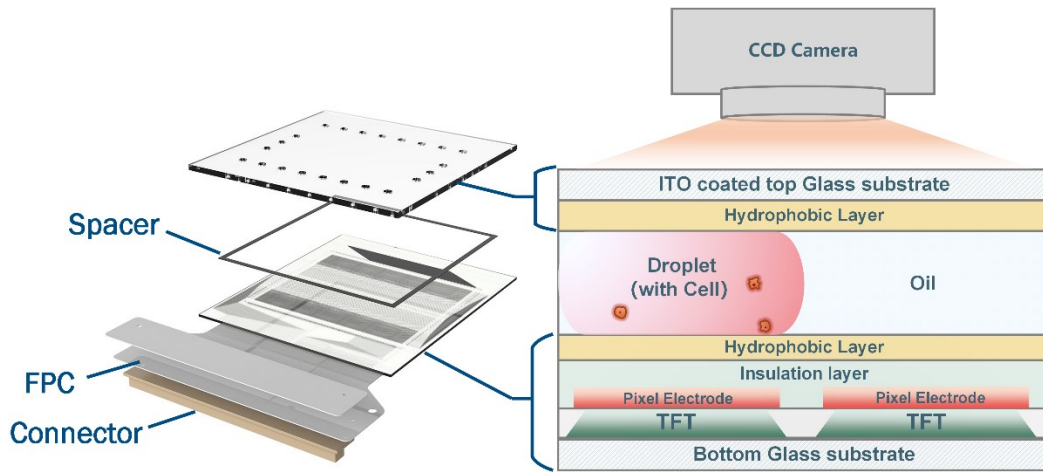


Fig S1 The structure and cross-section view of the AM-DMF chip



Fig S2 The software and hardware system setup of the AM-DMF chip



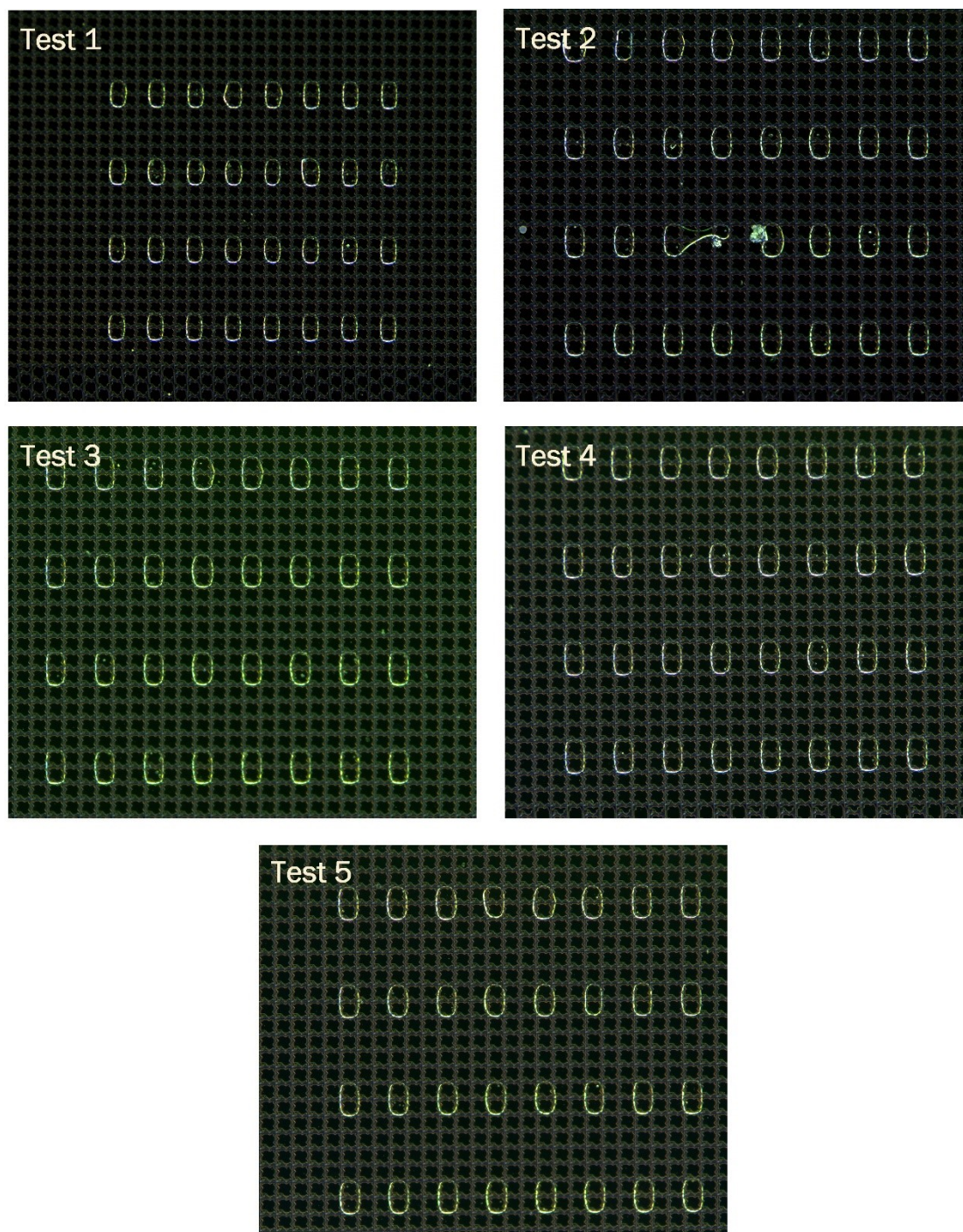


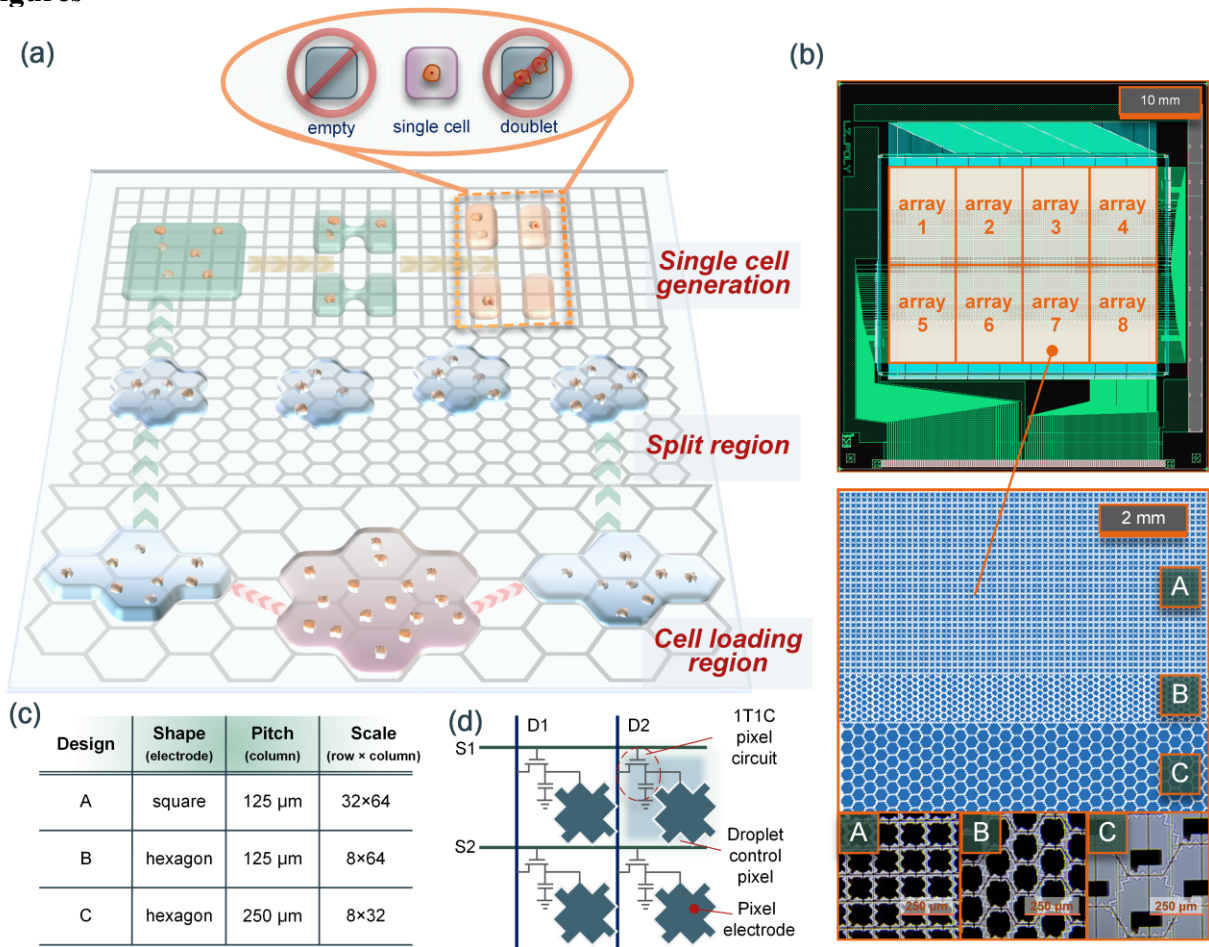
Fig S3 Single cell droplets generation experiment based on one-to-two method in the AM-DMF chip



Movie S1 Automated single cell droplets generation in the AM-DMF chip

Movie S2 The target single cell droplet movement in the AM-DMF chip

Figures



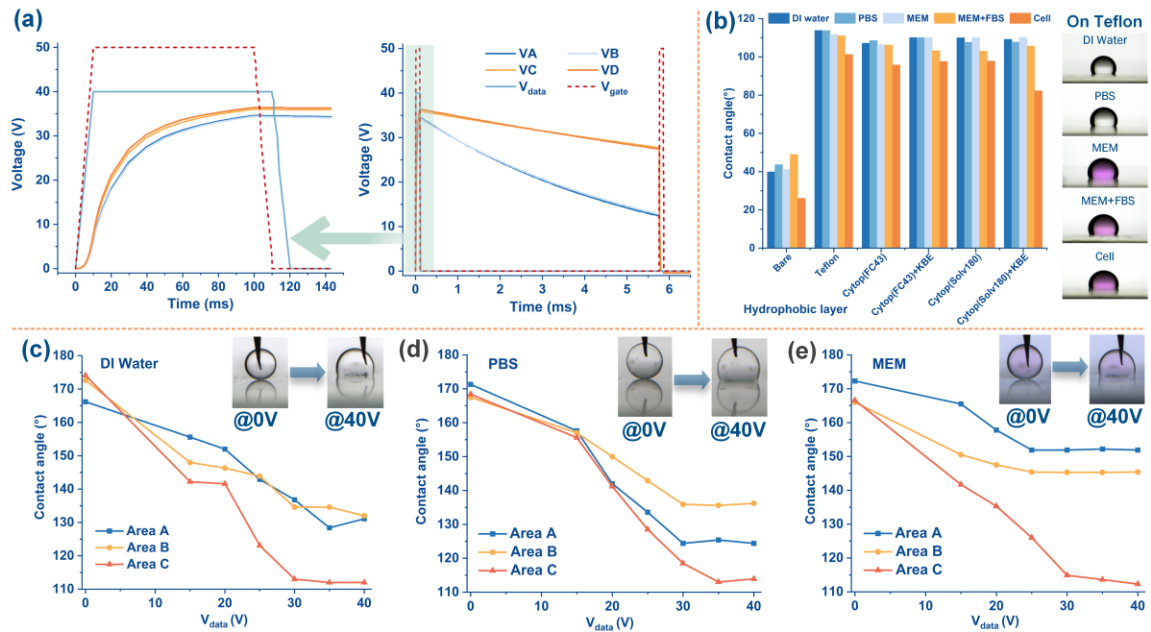


Fig. 2. (a) Pixel driving signals simulation with pixel charge and discharge, (b) The contact angles of different liquid reagents on the different hydrophobic layers, (c)-(e) The Contact angle of DI water, PBS buffer and MEM at various applied Data voltage.

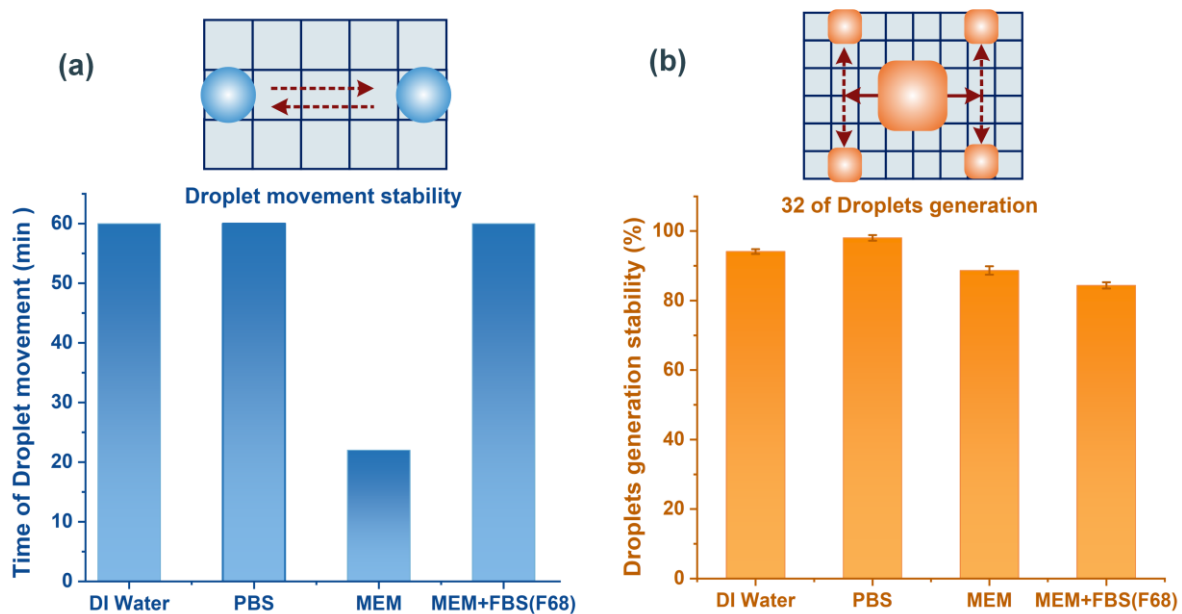
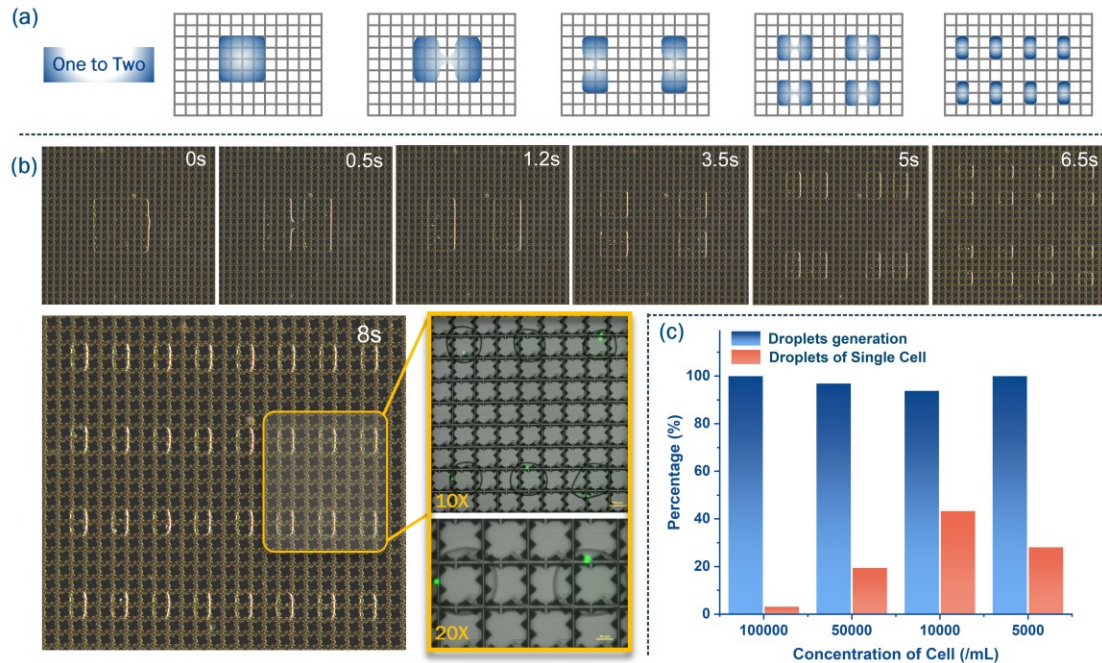
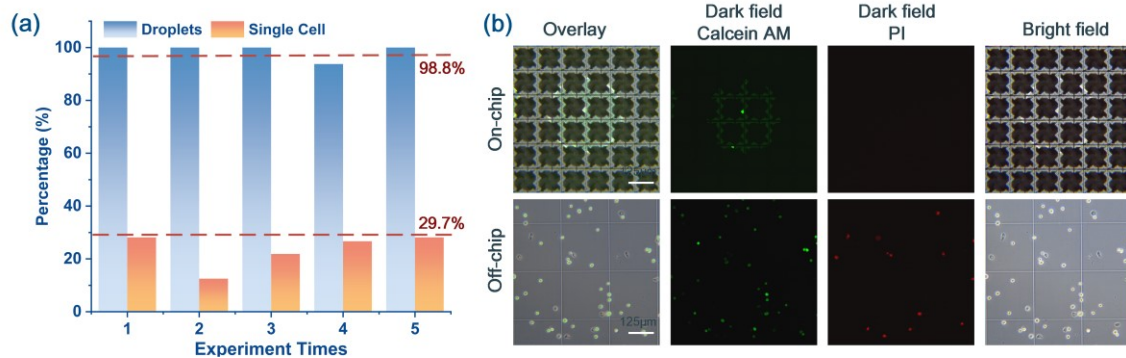


Fig. 3. The movement and generation stability of the droplet (a) For the stability test of droplet movement, the droplet continuously reciprocates on a row of 5 electrodes. (b) Stability test for the generation of 32 single droplets using a one-to-two approach



**Fig.4.** The single cell droplets generation on the AM-DMF chip. (a) Schematic diagram of the droplets generation path of One-to-Two method; (b) The screenshots of each step of the 32 droplet generation process and the fluorescence microscopic images of droplet; (c) The probability of generating the single cell droplet with different concentrations of cell reagent



**Fig.5.** The single cell generation and cell culture on the AM-DMF (a) Probability of cell solution to generate the droplets and single cell. (b) Cell viability test on and off-chip